Energy Efficient Autonomous Driving of Electric Vehicle with Real-Time Optimization Using Linear Quadratic Regulator

Mitsuhiro Hattori* Student Member, Hiroshi Fujimoto* Senior Member
Yoich Hori* Fellow, Yusuke Takeda** Non-member
Koji Sato** Non-member

Energy efficient driving of the electric vehicle is especially important in terms of range extension. In this paper, the optimization of energy consumption of the electric vehicle is considered. Optimization algorithms are generally divided into online and offline. Unlike offline, online optimization is a real-time optimization and can perform closed loop optimal control. Thus online optimization has an advantage in changing environments of the road while it requires fast computation.

In this paper, dynamic programming (DP) is used as an offline algorithm, and linear quadratic regulator (LQR) is proposed as an online algorithm. With approximations of some conditions, energy loss of electric vehicle is considered as cost function of LQR. By simulation and experiment, it is proven that proposed LQR is successfully applied to the optimization of energy consumption of an electric vehicle

Keywords: electric vehicle, energy efficient, autonomous driving, linear quadratic regulator

1. Introduction

1.1 Driver-Assistance System Over 1.2 million people die each year on road, and 20 to 50 million people suffer injuries [1]. To improve road transport safety, many devices have been developed, such as disk brakes, seat belts, and airbags.

In the 1990s, due to the improvement of sensors and computers, anti-lock braking systems (ABS), electronic stabilization programs (ESP) were developed [2]. With sensors of monitoring outside the vehicle, more assistance systems such as auto-braking and lane departure warning are also developed. These systems are called advanced driver-assistance systems (ADAS).

To maintain a safe, preset minimum distance between cars in the same lane, adaptive cruise control (ACC) was developed [3]. ACC is capable of improving not only road safety but also driver's comfort [4], and with string stability, traffic flow [5]. Since ACC enables autonomous car following without driver's input, it was shown that ACC can create more energy efficient driving experience [6].

1.2 Energy Efficient Driving Energy efficient drive technologies are important for three reasons, range extension, CO_2 emission, and running cost. Range extension is especially important for electric vehicles, whose cruising distance per supply is relatively shorter than gasoline vehicles [7]. From environmental aspects, CO_2 emissions have possibilities of great reductions by energy efficient drive, since 24% of the world's CO_2 emissions from fuel combustion is contributed by transportation sector [8].

Figure 1: Picture of FPEV-2 Kanon.

Furthermore, from an economical point of view, the energy efficiency of the vehicle leads to reduction of running cost, which is getting more dominant with sharing economy [9]. Achieving energy efficient driving is, therefore, getting more important.

As an energy efficient driving of electric vehicles, distribution of rear and front driving force of the electric vehicle was controlled [10]. with optimization, the velocity trajectory of the vehicle is also optimized [11]. In this paper, energy efficient driving is achieved by optimal velocity control.

1.3 Optimization Algorithm Optimization algorithms are generally divided into online and offline. Online optimization is a real-time optimization method which makes the decision without complete knowledge of the problem [12]. Offline optimization is an optimization method which performs optimization of the whole problem before the control

* The University of Tokyo
5–1–5, Kashiwanoha, Kashiwa, Chiba, 227–8561 Japan
** Ono Sokki Co.,Ltd.
3–9–3, Shin-Yokohama, Kohoku-ku, Yokohama, Kanagawa, 222–8507 Japan

© 2019 The Institute of Electrical Engineers of Japan.

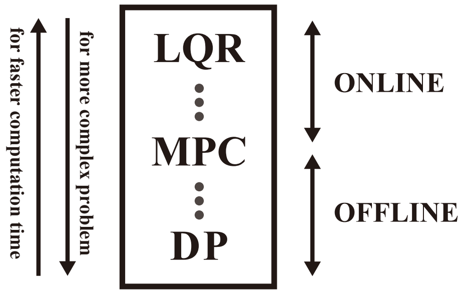

Figure 2: Comparison of optimization algorithms.

starts.

Control with online optimization is a closed loop optimal control and has an advantage in changing environments, but requires fast computation time. Offline optimization is proven to be effective on optimizing running profile of trains under fixed origin and destination [13]. For electric vehicles, however, control with offline optimization is limited to a certain condition because of a large number of running patterns [14]. In this paper, online optimization is considered and compared with offline optimization.

Figure 2 shows some of online and offline optimization algorithms.

Dynamic programming (DP) is an offline optimization algorithm which can solve complex problem with constraints. With DP, a large table of optimal inputs for certain condition is created, and by reading the table, the input is selected real-time [15]. The optimization process of DP, however, requires long computation time and is an offline optimization. Since optimizing every possible environmental change including other cars creates a very large table, it can be impractical to use it for electric vehicles [16].

Model predictive control (MPC) is an online optimal control algorithm with complex environmental changes and constraints. MPC is also used for optimizing energy consumption of vehicles [17, 18], but it is difficult to run optimization of MPC within the sampling period, because of the complexity of the optimization [19].

Linear quadratic regulator (LQR) is the simplest method of optimal control. Since it is solved merely with solving Riccati's equation, the computation time is quite short.

1.4 About this paper In this paper, DP is selected as an offline algorithm, and LQR is proposed as a practical online algorithm. With approximations of some conditions, it is made possible to apply LQR for reducing the energy consumption of an electric vehicle. The validity of the proposed LQR is presented as a comparison to DP by simulations and experiments with the vehicle. Experiments with Real Car Simulation Bench (RC-S) of Ono Sokki Co., Ltd., and experiments on the experimental field of Japan Automobile Research Institute (JARI) was performed to test the validity of the method. More result of the experiment is expected by final submission.

The reminder of this paper is organized as follows: Section 2 describes experimental vehicle and its model; Section 3 presents details of optimization algorithm, DP and LQR; Section 5 shows the result of simulation and experiment; Section 6 discusses the validity of the method; and Section 7 concludes this paper.

Table 1: Vehicle parameters (common).

Parameter	Description	Value
M	Vehicle mass	880 kg
g	Gravity acceleration	9.8 m/s^2
b	Viscous resistance coefficient	10.7 kg/s
r	Wheel radius	0.302 m
F_a	Air resistance coefficient	0.552 Ns^2/m^2
μ_r	Rolling resistance coefficient	0.0126
P	Number of pole pairs	20/2
h_g	Height of center of gravity (CG)	0.51 m
l_f	Distance between CG & front wheel	1.013 m
l_r	Distance between CG & rear wheel	0.702 m

Table 2: Vehicle parameters (front).

Parameter	Description	Value
J_ω	Wheel inertia	1.24 kgm^2
L_q	q-axis inductance	0.000 69 H
Φ	Leakage flux	0.18 Wb
R	Copper resistance	0.0602 Ω
R_{c0}	Equivalent iron loss resistance	55 Ω
R_{c1}	Equivalent iron loss resistance	0.14 Ω
K_t	Motor constant	2.7 Nm/A

2. Experimental Vehicle Model

2.1 Experimental Vehicle FPEV-2 Kanon, shown in Figure 1, is an experimental vehicle manufactured by authors' research group. This vehicle has four independently driven in-wheel motors, and the motor is an outer-rotor permanent magnet synchronous motor.

Since all in-wheel motors are direct-drive, the reaction force transfers to roads without the influence of gear backlash or shaft torsion. Therefore, only motor loss and driving resistance are considered as energy loss.

2.2 Motor Model The input power of the motor P_{in} is defined as the sum of output power P_{out}, copper loss P_c, and iron loss P_i. Each of them is defined as

$$P_{out} = \sum_{all} \omega T \qquad (1)$$

$$P_c = \sum_{all} R \left(\frac{T}{K_t} \right)^2 \qquad (2)$$

$$P_i = \sum_{all} \frac{\omega P}{R_c} \left\{ \left(L_q \frac{T}{K_t} \right)^2 + \Phi^2 \right\} \qquad (3)$$

where T and ω are torque and rotational speed, and equivalent iron loss resistance R_c is

$$\frac{1}{R_c} = \frac{1}{R_{c0}} + \frac{1}{R_{c1}|\omega P|} \qquad (4)$$

Parameters of the vehicle are shown in Table 1–3.

2.3 Vehicle Model The dragging force of the vehicle is described as

$$F_{DR} = \mu_r M g + b|v| + F_a v^2 \qquad (5)$$

where each term refers to rolling resistance, viscous resistance, and air resistance. Each parameter is shown in Table 1.

Load force of front and rear wheels is described as follows.

$$N_f = \frac{1}{2} \left(\frac{l_r}{l} M g - \frac{h_g}{l} M \dot{v} \right) \qquad (6)$$

Table 3: Vehicle parameters (rear).

Parameter	Description	Value
J_ω	Wheel inertia	1.26 kgm^2
L_q	q-axis inductance	0.002 34 H
Φ	Leakage flux	0.249 Wb
R	Copper resistance	0.1036 Ω
R_{c0}	Equivalent iron loss resistance	454.23 Ω
R_{c1}	Equivalent iron loss resistance	0.1516 Ω
K_t	Motor constant	1.245 Nm/A

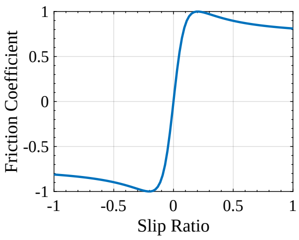

Figure 3: $\mu - \lambda$ curve.

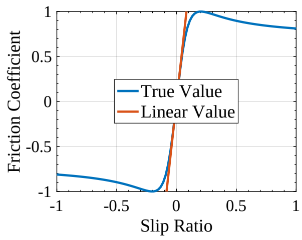

Figure 4: Driving stiffness.

$$N_r = \frac{1}{2}\left(\frac{l_f}{l}Mg + \frac{h_g}{l}M\dot{v}\right) \cdots\cdots (7)$$

In order to calculate driving force, slip ratio λ is defined as

$$\lambda = \frac{r\omega - v}{\max(v, r\omega)} \cdots\cdots (8)$$

where ω is wheel angular velocity. Using relation between road friction coefficient μ and slip ratio λ shown in Figure 3, driving force of each wheel is calculated as $F = \mu N$. The equation of rotational motion and equation of the vehicle motion are

$$J_\omega \dot{\omega} = T - rF \cdots\cdots (9)$$

$$M\dot{v} = \sum F - F_{DR} \cdots\cdots (10)$$

where T is torque and F is the driving force of each wheel.

3. Optimization Algorithm

3.1 Dynamic Programming Dynamic programming (DP) is a commonly used offline optimization algorithm especially in train [20].

In DP, the problem is divided into multiple subproblems and the optimization is solved efficiently with the results of subproblems. In order to apply DP in this problem, the problem is discretized by velocity and position. The model of motor power is changed as

$$P_{out} = \frac{1}{2}vF_{all}\sum\left(1 + \frac{F_{all}}{4D_sN}\right) \cdots\cdots (11)$$

$$P_c = \frac{r^2}{8}F_{all}^2\sum\frac{R}{K_t^2} \cdots\cdots (12)$$

$$P_i = 2\frac{v^2}{r^2}\sum\frac{P_n^2}{R_c}\left\{\left(\frac{rL_qF_{all}}{4K_t}\right)^2 + \Phi^2\right\} \cdots\cdots (13)$$

to calculate them from discretised velocity [21]. F_{all} is sum of the driving force and $D_s(= 12)$ is linearized coefficient of the relation between slip ration and tire friction. D_s is called driving stiffness and visualized in Figure 4.

In this paper, the the velocity of the vehicle is optimized. The evaluation function is energy consumption W_{in} which is time integration of $P_{in}(= P_{out} + P_c + P_i)$. In order to calculate optimized velocity for each position, the value of the goal is set to 0 if the velocity is 0 m/s, and set to ∞ if it is not.

Making a table of every value of evaluation function in each step by the result of the next step, the optimal velocity of each position is calculated with the table.

3.2 Linear Quadratic Regulator In this paper, the linear quadratic regulator (LQR) is used as the simplest online optimal control. To apply LQR, the equation of vehicle motion is simplified as

$$M\dot{v} = F_{all} - Bv = \frac{4K_t i}{r} - Bv \cdots\cdots (14)$$

B is a linearized driving resistance defined as

$$F_{DR} = \mu_r Mg + b|v| + F_a v^2 \approx A + Bv \cdots\cdots (15)$$

Motor power model is simplified as

$$L\frac{di}{dt} = V - Ri - K_e\omega = V - Ri - K_e\frac{v}{r} \cdots\cdots (16)$$

which ignores iron loss and tire slip.

Calculating $(14) \times v + (16) \times 4i$ and assuming $K_t = K_e$ lead

$$\frac{d}{dt}\left(\frac{1}{2}Mv^2 + 4\frac{1}{2}Li^2\right) = 4Vi - (4Ri^2 + Bv^2) \cdots\cdots (17)$$

The right side of (17) consists of output power Vi, copper loss Ri^2, and driving resistance Bv^2. Thus the objective should be minimizing the loss term $(4Ri^2 + Bv^2)$.

In LQR, the system is described as

$$\frac{d\boldsymbol{x}}{dt} = \begin{pmatrix} 0 & 1 \\ 0 & -\frac{B}{M} \end{pmatrix}\boldsymbol{x} + \begin{pmatrix} 0 \\ \frac{4K_t}{rM} \end{pmatrix}\boldsymbol{u} \cdots\cdots (18)$$

where state $\boldsymbol{x} = (p \quad v)^T$ consists of position and velocity, and input $\boldsymbol{u} = i^*$ is motor current reference assuming the current control is ideal.

The evaluation function of LQR is

$$J(\boldsymbol{u}) = \int_0^\infty (\boldsymbol{x}^T\boldsymbol{Q}\boldsymbol{x} + \boldsymbol{u}^T\boldsymbol{R}\boldsymbol{u})dt \cdots\cdots (19)$$

and by setting $\boldsymbol{Q}$ and $\boldsymbol{R}$ as

$$\boldsymbol{Q} = \begin{pmatrix} q & 0 \\ 0 & B \end{pmatrix}, \quad \boldsymbol{R} = 4R \cdots\cdots (20)$$

the function to be integrated is made to be

$$qp^2 + Bv^2 + 4Ri^2 \cdots\cdots (21)$$

Thus, the minimization of the evaluation function is equivalent to the minimization of the loss.

In this case, the only parameter to be tuned is q. It is required to reduce offset of the position. Considering the friction of the road, the relation between the offset and q is simulated, and the relation between the value of energy loss $Bv^2 + 4Ri^2$ and q is also simulated. The relations are shown in Figure 5. Larger q results in smaller offset value but leads to more energy consumption.

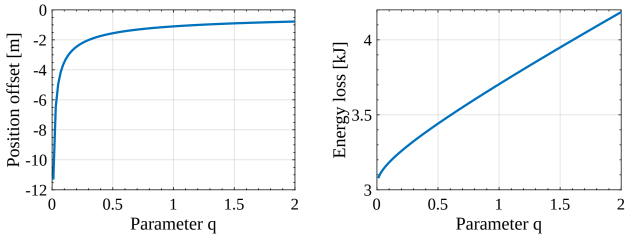

(a) Position offset. (b) Energy loss.

Figure 5: Simulation of the effect of changing q.

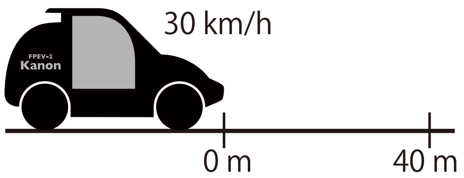

Figure 6: Problem establishment.

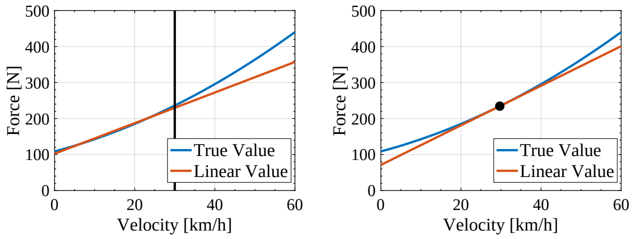

(a) Proposal 1. (b) Proposal 2.

Figure 7: Approximations of driving resistance.

4. Methods

4.1 Problem Establishment The problem establishment for comparison is a simple decelerating situation shown in Figure 6. The vehicle of 30 km/h decelerates and stops at 40 m.

In this decelerating situation, the objectives are to maximize regenerative energy and to minimize energy consumption.

4.2 Proposal methods The proposal methods are divided into two methods. Both methods are based on the LQR, The difference is the way how driving resistance is approximated. Proposal 1 approximates driving resistance in used velocity range with least square method, and proposal 2 linearizes it around each operating point. For proposal 2, linearized driving resistance is described as

$$B = b + 2F_a v' \quad (22)$$

where v' is the velocity of the operating point. Each approximation is shown in Figure 7. For time variant resistance of proposal 2, the same steady state Riccati's equation is used and the computation time is same as proposal 1.

4.3 Controller For DP, velocity controller to follow calculated velocity is designed and shown in Figure 8. λ^* is set to 0.05, and gain of PI controller is set as $K_p = 10M$, $K_i = -25M$. The gain is designed to place pole to -5 rad/s for plant $sMV = F$. For LQR, feedback controller of velocity and position is designed. Figure 9 shows the controller of LQR.

5. Result

5.1 Simulation Result In order to simulate LQR and DP equally, full vehicle model of experimental vehicle is used. This model has tire model with slip ratio and motor characteristic and vehicle model with load distribution of four wheels. Autonomous vehicle control of each optimization algorithm is simulated with this model and compared in terms of energy consumption.

For simulation, deceleration with constant acceleration control is also simulated. In this case, parameter q is tuned with the relation shown in Figure 5, and set to 1.0.

The comparison of each methods is shown in Figure 10. In Figure 10, Conv. refers to the deceleration with constant acceleration control, and DP refers to the control with dynamic programming. Prop.1 and Prop.2 refer to the control with LQR.

Compared with constant acceleration control, DP and LQR are more than 3% better in regenerative energy. LQR with time variant parameter regenerate energy more than constant parameter LQR.

5.2 Experimental Result of Bench Test Real Car Simulation Bench (RC-S) is an instrument for bench tests using an actual vehicle. Since RC-S absorbs driving force by directly connecting driving wheels to a dynamometer, it is possible to test electric vehicle with fast reaction with RC-S [22].

For experiment with bench test, experimental vehicle FPEV-2 Kanon is used. The velocity of the vehicle is taken from the calculated value of RC-S. For each condition, the experiment is performed 5 times and standard error of energy consumption is calculated.

Experimental result of bench test is shown in Figure 11. DP refers to the control with dynamic programming. Prop.1 and Prop.2 refer to the control with LQR. In this case, parameter q is tuned to the same value as simulation.

Prop.2 regenerates energy more than DP in this bench test, but vehicle position did not reach 40 m with Prop.2. Same as simulation result, LQR with time variant parameter regenerate energy more than constant parameter LQR.

5.3 Experimental Result of Field Test As an experiment with the vehicle, FPEV-2 Kanon is used in the test field. For each condition, the experiment is performed 5 times and standard error of energy consumption is calculated. By ignoring wheel slip of the vehicle, the velocity of the vehicle is taken from the wheel resolver. Experimental result of field test is shown in Figure 12–14.

Figure 12 and Figure 13 are results of deceleration from 30 km/h with different parameter q. Figure 14 is the result of deceleration from 45 km/h with distance of 60 m. Same as simulation result and bench test, LQR with time variant parameter regenerate energy more than constant parameter LQR.

6. Discussion

From simulation result, proposed methods are proven to be sufficiently better than constant acceleration control. In bench test, the regenerative energy of Prop.2 is better than that of DP, but it is because the travel distance was shorter than that of DP.

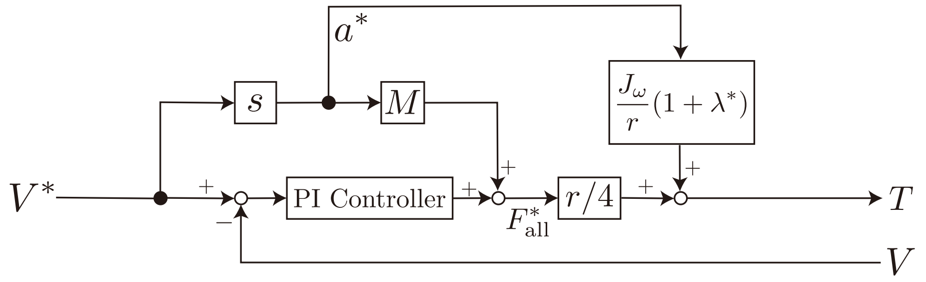

Figure 8: Controller for DP.

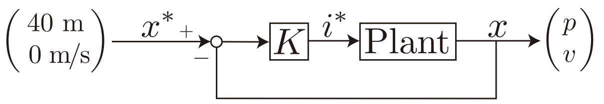

Figure 9: Controller for LQ.

From experimental result with different parameter and different velocity, Prop.2 is shown better than Prop.1 in regenerative energy. The difference of values of regenerative energy is caused by offset of current sensors and road condition. While computation time of DP was more than 5 minutes just for this limited condition, proposed LQR computed online with 10 kHz of control cycle. Considering the fact that no algorithm can surpass the result of DP, proposed methods are valid for optimizing energy consumption of electric vehicle.

7. Conclusion

Various optimization algorithms with various computation time are used for optimization of energy consumption of vehicles. In this paper, the offline optimization algorithm DP and proposed LQR are compared in terms of energy consumption. With approximations of some conditions, energy loss of electric vehicle is considered as cost function of LQR, and LQR is successfully applied to the optimization of energy consumption of an electric vehicle. Time variant approximation is conducted as Prop.2 and proven better with same computation time. The simulation and experimental result supports the fact that the LQR is a valid method. As a future work, comparison with more complicated optimal control algorithms is needed.

Acknowledgment

This research was partly supported by Industrial Technology Research Grant Program from New Energy and Industrial Technology Development Organization (NEDO) of Japan (number 05A48701d), the Ministry of Education, Culture, Sports, Science and Technology grant (number 18H03768 and 26249061), and JST CREST Grant Number JPMJCR15K3, Japan.

References

(1) World Health Organization: "Global status report on road safety: Summary", Technical report (2009).

(2) G. Leen and D. Heffernan: "Expanding Automotive Electronic Systems", Computer, **35**, 1, pp. 88–93 (2002).

(3) W. D. Jones: "Building safer cars", IEEE Spectrum, **39**, 1, pp. 82–85 (2002).

(4) M. Hoedemaeker and K. A. Brookhuis: "Behavioural adaptation to driving with an adaptive cruise control (ACC)", Transportation Research Part F: Traffic Psychology and Behaviour, **1**, pp. 95–106 (1998).

(5) C.-Y. Liang and H. Peng: "String Stability Analysis of Adaptive Cruise Controlled Vehicle", JSME International Journal Series C, **43**, 3, pp. 671–677 (2000).

(6) K. J. Malakorn and B. Park: "Assessment of Mobility, Energy, and Environment Impacts of IntelliDrive-based Cooperative Adaptive Cruise Control and Intelligent Traffic Signal Control", IEEE International Symposium on Sustainable Systems and Technology, pp. 1–6 (2010).

(7) C. C. Chan: "The State of the Art of Electric, Hybrid, and Fuel Cell Vehicles", Proceedings of the IEEE, **95**, 4, pp. 704–718 (2007).

(8) I. E. A. IEA: "CO2 Emissions from Fuel Combustion Highlights", Technical report (2017).

(9) F. Bardhi and G. M. Eckhardt: "Access-Based Consumption : The Case of Car Sharing", Journal of Consumer Research, **39**, pp. 881–898 (2012).

(10) S. Harada and H. Fujimoto: "Range Extension Control System for Electric Vehicles during Acceleration and Deceleration Based on Front and Rear Driving-Braking Force Distribution Considering Slip Ratio and Motor Loss", IECON 2013 - 39th Annual Conference of the IEEE Industrial Electronics Society, pp. 6626–6631 (2013).

(11) Y. Ikezawa, H. Fujimoto, Y. Hori, D. Kawano, Y. Goto, M. Tsuchimoto and K. Sato: "Range Extension Autonomous Driving for Electric Vehicles Based on Optimal Velocity Trajectory Generation and Front-Rear Driving-Braking Force Distribution", IEEJ Journal of Industry Applications, **5**, 3, pp. 228–235 (2016).

(12) S. O. Krumke and C. Thielen: "Introduction to Online Optimization" (2014).

(13) H. Ko, T. Koseki and M. Miyatake: "Application of dynamic programming to the optimization of the running profile of a train", Computers in Railways IX, pp. 103–112 (2004).

(14) N. Ogawa, H. Fujimoto, N. Okui, Y. Takeda and K. Sato: "Range Extension Autonomous Driving for Electric Vehicles Considering Uncertainty of Signal Information", IEEJ International Workshop on Sensing, Actuation, Motion Control, and Optimization, pp. 1–6 (2018).

(15) H. Ko, T. Koseki and M. Miyatake: "Numerical Study on Dynamic Programming Applied to Optimization of Running Profile of a Train", IEEJ Transactions on Industry Applications, **125**, 12, pp. 1084–1092 (2005).

(16) V.-D. Doan, H. Fujimoto, T. Koseki, T. Yasuda, H. Kishi and T. Fujita: "Iterative Dynamic Programming for Optimal Control Problem with Isoperimetric Constraint and Its Application to Optimal Eco-driving Control of Electric Vehicle", IEEJ Journal of Industry Applications, **7**, 1, pp. 80–92 (2018).

(17) B. Sakhdari and N. L. Azad: "A Distributed Reference Governor Approach to Ecological Cooperative Adaptive Cruise Control", IEEE Transactions on Intelligent Transportation Systems, **19**, 5, pp. 1496–1507 (2018).

(18) A. Weißmann, D. Görges and X. Lin: "Energy-optimal adaptive cruise control combining model predictive control and dynamic programming", Control Engineering Practice, **72**, November 2017, pp. 125–137 (2018).

(19) S. Xu and H. Peng: "Design and Comparison of Fuel-Saving Speed Planning Algorithms for Automated Vehicles", IEEE Access, **6**, pp. 9070–9080 (2018).

(20) N. Ghaviha, M. Bohlin, F. Wallin and E. Dahlquist: "Optimal Control of an EMU Using Dynamic Programming", Energy Procedia, Vol. 75, Elsevier B.V., pp. 1913–1919 (2015).

(21) T. Fukuda, H. Fujimoto, Y. Hori, D. Kawano, Y. Goto, Y. Takeda and K. Sato: "Basic Study on Range Extension Autonomous Driving of Electric Vehicle Considering Velocity Constraint for Real-Time Implementation", IEEJ International Workshop on Sensing, Actuation, Motion Control, and Optimization, pp. 1–6 (2017).

(22) Y. Goto, D. Kawano, K. Sato and K. Echigo: "Analysis of Behavior of Fuel Consumption and Exhaust Emissions under On- road Driving Conditions Using Real Car Simulation Bench (RC-S)", SAE International Journal of Engines, **2**, 2, pp. 611–616 (2009).

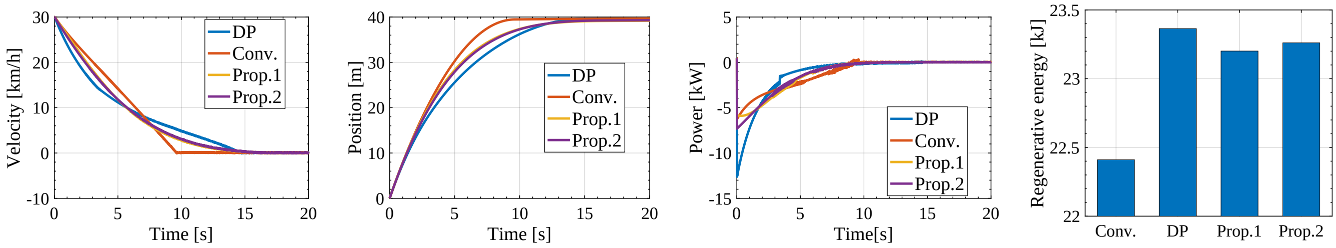

(a) Velocity trajectory. (b) Vehicle position. (c) Inverter input power. (d) Regenerative energy.

Figure 10: Simulation result (30 km/h, 40 m, q = 1).

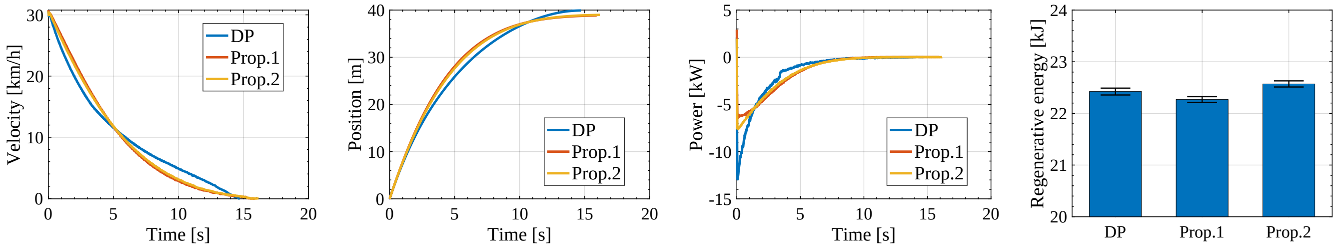

(a) Velocity trajectory. (b) Vehicle position. (c) Inverter input power. (d) Regenerative energy.

Figure 11: Experimental result of bench test (30 km/h, 40 m, q = 1).

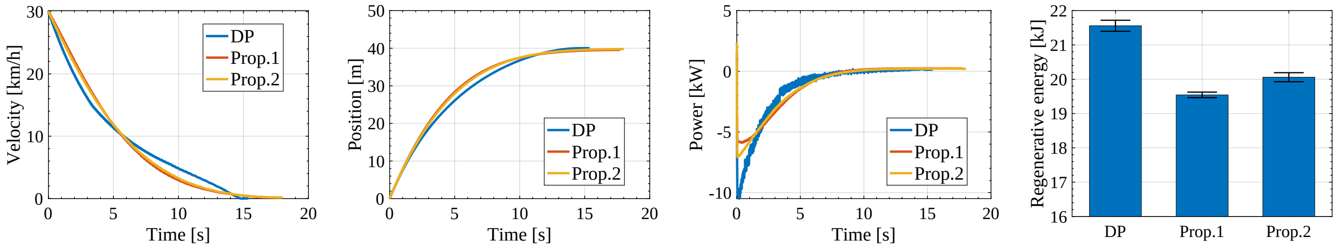

(a) Velocity trajectory. (b) Vehicle position. (c) Inverter input power. (d) Regenerative energy.

Figure 12: Experimental result of field test (30 km/h, 40 m, q = 1).

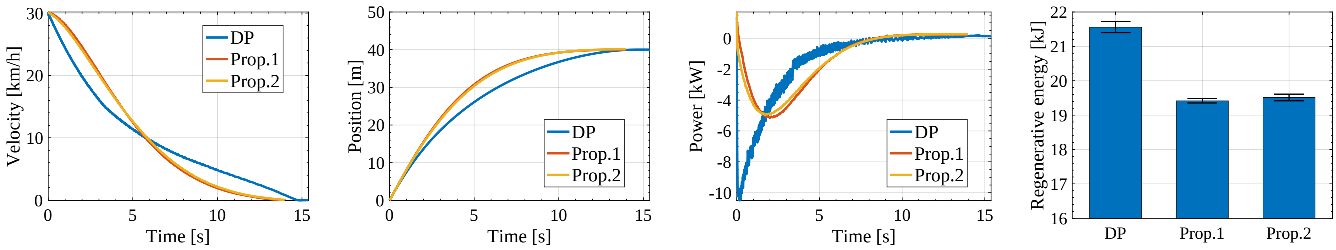

(a) Velocity trajectory. (b) Vehicle position. (c) Inverter input power. (d) Regenerative energy.

Figure 13: Experimental result of field test (30 km/h, 40 m, q = 2).

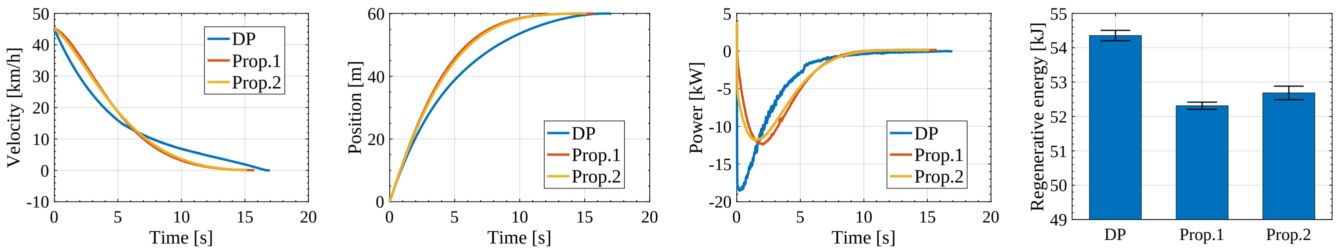

(a) Velocity trajectory. (b) Vehicle position. (c) Inverter input power. (d) Regenerative energy.

Figure 14: Experimental result of field test (45 km/h, 60 m, q = 2).